Catalytic and substrate promiscuity: distinct multiple chemistries catalysed by the phosphatase domain of receptor protein tyrosine phosphatase

Bharath Srinivasan*, Hanna Marks*, Sreyoshi Mitra*, David M. Smalley† and Jeffrey Skolnick*[1]

*Center for the Study of Systems Biology, School of Biology, Georgia Institute of Technology, 950, Atlantic Drive, Atlanta, GA 30332, U.S.A.
†Systems Mass Spectrometry Core (SyMS-C), Georgia Institute of Technology, 950 Atlantic Drive, Atlanta, GA 30318, U.S.A.

The presence of latent activities in enzymes is posited to underlie the natural evolution of new catalytic functions. However, the prevalence and extent of such substrate and catalytic ambiguity in evolved enzymes is difficult to address experimentally given the order-of-magnitude difference in the activities for native and, sometimes, promiscuous substrate/s. Further, such latent functions are of special interest when the activities concerned do not fall into the domain of substrate promiscuity. In the present study, we show a special case of such latent enzyme activity by demonstrating the presence of two mechanistically distinct reactions catalysed by the catalytic domain of receptor protein tyrosine phosphatase isoform δ (PTPRδ). The primary catalytic activity involves the hydrolysis of a phosphomonoester bond (C—O—P) with high catalytic efficiency, whereas the secondary activity is the hydrolysis of a glycosidic bond (C—O—C) with poorer catalytic efficiency. This enzyme also displays substrate promiscuity by hydrolysing diester bonds while being highly discriminative for its monoester substrates. To confirm these activities, we also demonstrated their presence on the catalytic domain of protein tyrosine phosphatase Ω (PTPRΩ), a homologue of PTPRδ. Studies on the rate, metal-ion dependence, pH dependence and inhibition of the respective activities showed that they are markedly different. This is the first study that demonstrates a novel sugar hydrolase and diesterase activity for the phosphatase domain (PD) of PTPRδ and PTPRΩ. This work has significant implications for both understanding the evolution of enzymatic activity and the possible physiological role of this new chemistry. Our findings suggest that the genome might harbour a wealth of such alternative latent enzyme activities in the same protein domain that renders our knowledge of metabolic networks incomplete.

Key words: catalytic promiscuity, glycosidic bond, phosphoester bond, protein tyrosine phosphatase, substrate promiscuity.

INTRODUCTION

Numerous studies have demonstrated and discussed the evolutionary implications of catalytic promiscuity and the degeneracy of substrate preferences by enzymes [1–4]. Jensen [5] proposed that modern day enzymes, often assumed to be highly specialized for the reactions that they catalyse, have evolved from broad specificity ancestors. Further, instances of promiscuity have been extensively reported from members belonging to the haloacid dehalogenase superfamily [1,6], thioesterases from the hotdog fold superfamily [1] and others [7,8]. Demonstration of the limited number of distinct ligand-binding pockets and the emergence of catalytic pockets in proteins without selection for function has further strengthened the understanding that promiscuity and catalysis are inherent features of proteins and that it is very likely (and certainly not surprising) that the tremendous rate accelerations that we see with present day enzymes results from evolutionary selection from a significant random background [9,10]. However, it has been pointed out that most of these promiscuous secondary activities emerge from the same pocket with Nature utilizing the same microenvironment optimized to enhance catalytic potential [2]. There are very few previous studies that have attempted to characterize activities that are mechanistically distinct and, possibly, emerge from distinct pockets on the protein's surface. The reason for this paucity stems from both technical limitations (different assay systems and possible order-of-magnitude differences in the rates of the primary and the secondary activities) and the lack of a rational framework to search for such secondary activities. In the present paper, motivated by our computational work which strongly suggests that the likelihood of finding low level secondary enzymatic function is high, we demonstrate that the phosphatase domain (PD) of receptor protein tyrosine phosphatases (PTPRs) catalyses the hydrolysis of glycosidic (COC) bonds apart from its primary activity of cleaving phosphomonoester (COP) bond. This is important because the hydrolysis of COC bond in β-galactosides and COP bond in phosphomonoesters require different functional groups and different mechanism of cleavage [11,12].

PTPRs are a family of cell surface receptor proteins that antagonize tyrosine kinase signalling. The phosphatase domain of PTPRs catalyse a two-step phosphate monoester hydrolysis reaction through a highly conserved sequence motif (H/V)CX_5R(S/T) with a nucleophilic cysteine. PTPR subtype δ has a cell adhesion extracellular domain and two cytoplasmic protein tyrosine phosphatase (PTP) domains [13,14]. Protein tyrosine phosphatase δ (PTPRδ) is predominantly expressed in the brain and is known to be involved in the guidance and termination of motor neurons during embryonic development [15,16]. PTPRδ knockout mice exhibit impaired learning and memory, also indicating that PTPRδ is essential for the organization of neural

Abbreviations: NEM, *N*-ethylmaleimide; 4NGA-α, *p*-nitrophenyl α-D-galactoside; 4NGU-α, *p*-nitrophenyl α-D-glucoside; 4NP-NA-GU, *p*-nitrophenyl *N*-acetyl-β-D-glucosaminide; ONPG, *O*-nitrophenyl β-galactopyranoside; PD, phosphatase domain; PD-PTPRδ, phosphatase domain of PTPRδ; PD-PTPRΩ, phosphatase domain of PTPRΩ; PNPG, *p*-nitrophenyl β-galactoside; PNPGlucu, *p*-nitrophenyl β-glucuronide; pNPP, *p*-nitrophenyl phosphate; PTPR, receptor protein tyrosine phosphatases; PTPRδ, protein tyrosine phosphatase δ; PTPRΩ, protein tyrosine phosphatase Ω.

[1] To whom correspondence should be addressed (email skolnick@gatech.edu).

circuits [17]. The above observations, coupled with the knowledge that PTPRσ is a chondroitin sulfate (CS) receptor that propagates chrondritin sulfate proteoglycan (CSPG)-mediated inhibition and heparin sulfate proteoglycan (HSPG)-mediated axon outgrowth [18] and shares almost 77 % sequence identity with PTPRδ, makes one speculate that the role the two PTPRs exert in neuronal growth might be inextricably interlinked with recognition and processing of sugar moieties alongside phosphate moieties.

In the present paper, we report a novel sugar hydrolase activity in the PD of PTPRδ. Furthermore, the enzyme also displays substrate promiscuity by hydrolysing the diester bond while showing a high-level of discrimination in its primary monoesterase substrate preference. Compared with its primary phosphatase activity, the newly identified sugar hydrolase activity shows marked differences vis-à-vis rate enhancement, pH optima, metal-ion dependence and susceptibility to inhibitors. Further, this novel activity assumes significance since PTPRδ is predominantly expressed in the brain and is involved in guiding and termination of motor neurons during embryonic development. Since glycosaminoglycans, a family of linear sulfated polysaccharides, play important roles in neuronal growth, regeneration and plasticity [19], their sugar hydrolase activity may not be accidental and may indicate an important physiological role that this phosphatase plays vis-à-vis nerve growth. Finally, this work suggests that unexplored promiscuous activities may constitute an important pool of chemistries, deduction of which would help unravel the complexities of metabolism.

EXPERIMENTAL

Reagents

All reagents and chemicals, unless mentioned otherwise, were of high quality and were procured from Sigma–Aldrich, Amresco and Fisher Scientific. Media components were from Amresco. Macrosep centrifugal devices were from Pall Co. The expression clones for the phosphatase domain of PTPRδ (RnCD00383366) and PTPRΩ (HsCD00423639) were procured from DNASU plasmid repository, Arizona State University. The identity of the supplied clones was confirmed by DNA sequencing.

Bioinformatics analysis

The sequences of r-PTPRδ and other PTPRs were obtained from NCBI. The non-redundant database at NCBI was used to search for homologues of PTPRδ using the algorithm BLASTP. Distant homology searches were carried out using PSI-BLAST [20]. T-Coffee [21] was used for generating multiple sequence alignment profiles. Phylogenetic and molecular evolutionary analyses were done using MEGA, version 3.1 [22]. Molecular visualization and structure analysis were done using various tools like SPDBV [23], PyMOL (pymol.sourceforge.net) and CCP4 suite of programs [24].

Expression and purification

The expression plasmids were transformed into *Escherichia coli* DH5α cloning strain for the purpose of routine plasmid isolation and *E. coli* BL21 (DE3) for expression. The transformed cells were grown in terrific broth with kanamycin (50 μg/ml) as the selection marker and induced with IPTG at a final concentration of 0.3 mM. Induction was carried out at 17 °C for 8 h. The cells were pelleted down at 2600 × ***g*** for 20 min and were resuspended in 30 ml of lysis buffer (50 mM Tris/HCl, pH 7.4, 100 mM NaCl, 2 mM DTT and 10 % glycerol). The cells were lysed using a sonicator (40 % amplitude, 3 s on 5 s off for 35–40 cycles) yielding crude extract (CE) that was centrifuged at 12900 × ***g*** for 30 min. The supernatant (referred to as the soluble fraction, SE) was kept for binding with equilibrated nickel nitrilotriacetic acid (Ni-NTA) beads (Perfectflow Ni-NTA superflow 5-Prime GmbH) for 3 h whereas the pellet, representing the in-soluble fraction (ISF), and beads (BE) were stored to assess possible loss of protein on SDS/PAGE gel. After 3 h, the beads with the protein of interest was pelleted down and the flow-through containing *E. coli* background protein was collected to test on SDS/PAGE gel (FT). The beads were washed extensively with 30 ml of wash buffer (lysis buffer containing 0, 15 and 20 mM imidazole, respectively) (W-I, W-II and W-III fractions in Figure 1A). The bound enzyme was eluted with 5 ml of elution buffer (lysis buffer containing 250 mM imidazole). After the elution of the protein from Ni-NTA beads (E), EDTA was added to a final concentration of 1 mM to prevent oxidation by trace nickel contamination. The protein was concentrated to required volume using Macrosep centrifugal devices (Pall Co.) with 10 kDa cutoff membrane and stored at − 80 °C. SDS/PAGE analysis was performed using standard protocols [25]. Protein concentrations were determined by the method of Bradford [26] with BSA as a protein standard.

Protein purity assessment

The purity of the protein preparation was assessed by overloading the protein on an SDS/PAGE and by performing mass-spectrometric analysis on a Q Exactive™ Plus Mass spectrometer. The latter instrument is designed for accurate quantification of low-abundance analytes and superior trapping of large molecules for improved analysis of intact proteins.

For intact mass determination of phosphatase domain of PTPRδ (PD-PTPRδ), the protein was processed as follows. The recombinantly expressed and purified protein was extensively dialysed into 10 mM ammonium acetate using Sartorius Vivacon 500 microfiltration devices (2000 molecular mass cut-off filters) to remove nonvolatile salts and glycerol. It was then resuspended at a concentration of 300 ng/μl in 50 % acetonitrile/49 % water/1 % acetic acid for direct infusion into a Q Exactive™ Plus Mass spectrometer (Thermo Scientific) via the HESI-II source (Thermo Scientific). The instrument was operated in positive ESI mode with a sheath gas flow of 12 units, auxiliary gas of 3 units and no sheath gas flow, a spray voltage of 5.0 kV and a capillary temperature of 285 °C. The automatic gain control (AGC) targets of 1×10^6 with a maximum injection time of 200 ms, and 5 microscans were combined per spectrum. Spectra were averaged using Qual Browser Ver. 3.0.63 (Thermo Scientific) and deconvoluted manually. The mass-spectrometric analysis was repeated thrice with three independent batches of protein.

Activity measurements using pNPP as the substrate

To determine the kinetic parameters of the phosphatase activity for PD-PTPRδ and PD-PTPRΩ (phosphatase domain of PTPRΩ), the rate of *p*-nitrophenyl phosphate (pNPP) (Sigma) hydrolysis was determined by monitoring the increase in absorbance at 405 nm for 300 s. A molar absorption coefficient (ε) of 18000 $M^{-1} \cdot cm^{-1}$ for *p*-nitrophenol at 405 nm was used to compute the amount of product formed from the slope of initial velocity curves [27]. The non-enzymatic hydrolysis of pNPP was normalized by monitoring the reaction in a double beam Hitachi U-2010 UV–Vis spectrophotometer (Hitachi High Technologies America) with

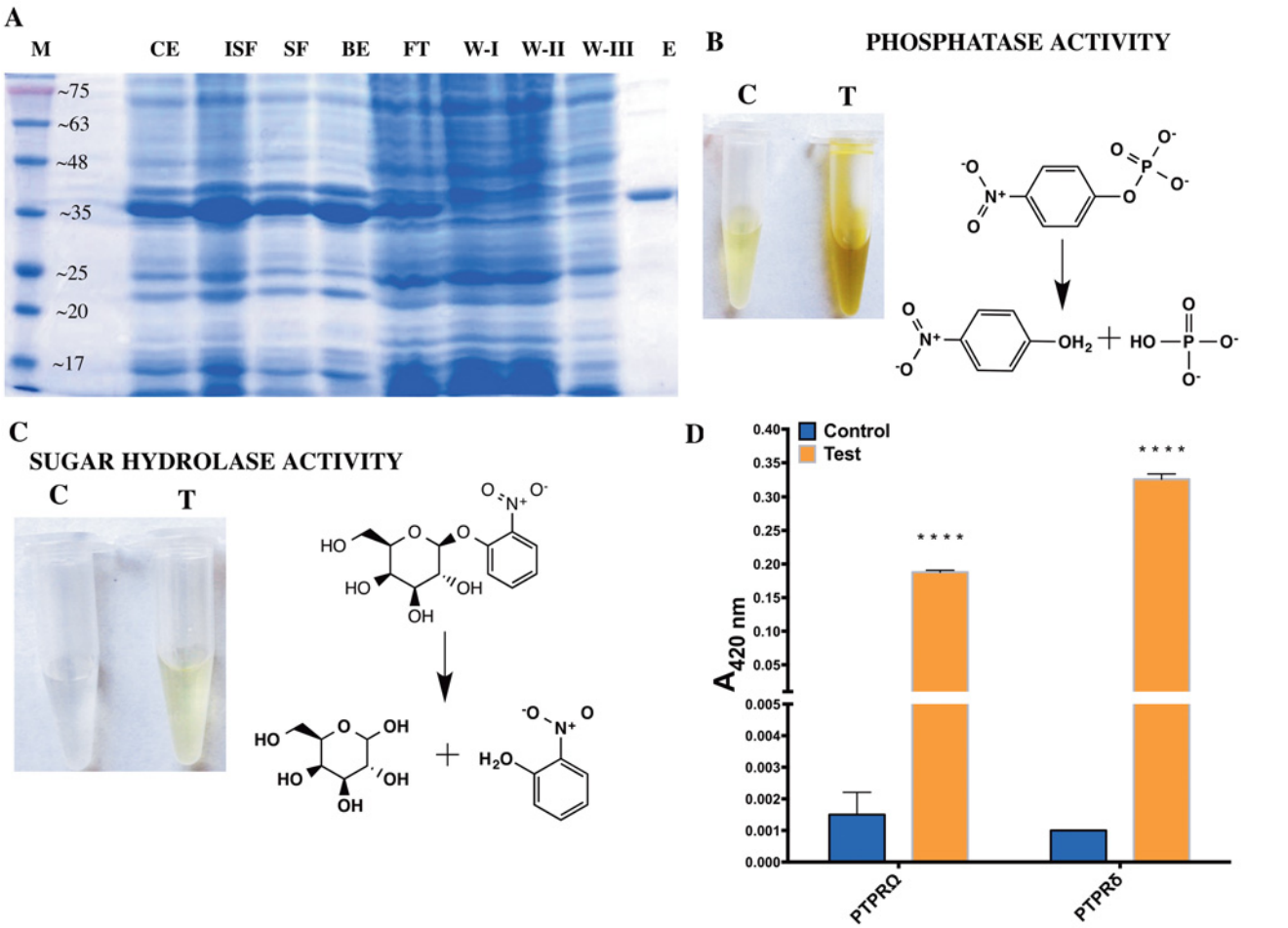

Figure 1 Protein purification and activity screen

(**A**) Expression and purification profile of the phosphatase domain of PTPRδ. The protein was purified to homogeneity using IMAC purification. The gel image shows the systematic purification of the recombinantly expressed protein from proteins in the *E. coli* cell lysate. M: molecular mass marker; CE: post-induction crude extract; ISF: in-soluble fraction; SF: soluble fraction; BE: Ni-NTA beads; FT: flow-through; W-I, -II, -III: Wash I, II and III, respectively. The numbers on the marker lane (M) indicates the molecular mass of the protein in KDa. (**B**) Assessment of phosphatase activity for the PD-PTPRδ. The substrate employed is pNPP and the reaction was allowed to proceed for 18 min at 37 °C. (**C**) Assessment of sugar hydrolase activity for the PD-PTPRδ. The substrate employed is *o*-nitrophenyl phosphate and the picture shows the reaction after 18 h of incubation at 37 °C. (**D**) Hydrolysis of galactoside bond by PD-PTPRδ and PD-PTPRΩ as assessed on ONPG**.** Two-way ANOVA was carried out to assess whether the difference was significant. A *P*-value of <0.0001 is represented by '****' symbols. Notations 'C' and 'T' indicate control (without enzyme) and test (with enzyme), respectively and the reaction schemes were rendered with ChemBioDraw 14.0.

an appropriate blank. Assays were initiated with the addition of enzyme to the sample cuvette after zeroing the absorbance reading with respect to the reference cuvette. The initial velocities were measured for reaction mixtures containing 100 mM HEPES pH 7.3 at room temperature (~22 °C).

To determine the K_m and V_{max} for pNPP, the substrate was titrated and the resultant velocities were plotted against substrate concentration and fit to either eqn (1) for one-site binding hyperbola in the absence of any substrate inhibition or eqn (2) when substrate inhibition was seen.

$$d[P]/dt = (V_{max} \times [S])/(K_m + [S]) \quad (1)$$

$$d[P]/dt = V_{max}/(1 + K_m/[S] + [S]/K_{SI}) \quad (2)$$

where $d[P]/dt$ is the rate of product formation, V_{max} is the maximum velocity, [S] is the substrate concentration, K_m is the Michaelis–Menten constant for pNPP and K_{SI} is the substrate–inhibition constant.

All the measurements were performed in duplicate with two independent experiments done and the resulting error values are reported as their S.D. To rule out the effect of ionic strength interfering with phosphatase activity due to metal ion addition, Mg^{2+} ion was titrated at saturating pNPP, and it was demonstrated that the activity remains constant. The concentration of PD-PTPRδ and PD-PTPRΩ used was 58 nM for pNPP hydrolysis. Unless mentioned otherwise, all the data were fit using linear regression and non-linear curve fitting subroutines of GraphPad Prism, version 4.0 (GraphPad Software).

Phosphate estimation by Chen's assay

The assays were carried out under initial velocity conditions where the product formed was less than 5 % of the initial substrate concentration. 100 μl of reaction volume contained 100 mM HEPES, pH 7.3, 15 mM $MgCl_2$ and various concentrations of substrate. Various substrates including *o*-phosphotyrosine, AMP, IMP, GMP, NADPH and pyridoxal 5′-phosphate were tested

Table 1 Substrate screen for PD-PTPRδ and PD-PTPRΩ

*'Yes' indicates significant increase in activity in the test (+ enzyme) with respect to the control reaction (− enzyme) as assayed calorimetrically in an end point assay or a continuous assay. 'No' indicates no significant difference in the test activity (with enzyme) with respect to the control reaction (no enzyme). Significance was assessed by performing a *t*-test. †Chen's assay for liberated phosphate. The assay conditions were 100 mM HEPES pH 7.3, 20 mM $MgCl_2$, 20 mM of IMP, AMP, GMP and pNPP, 10 mM PLP and 5 mM NADP, in 100 μl reaction mixture. The assay was incubated for 30 min, quenched with 70 % TCA and the reaction mixture was added to Chen's reagent for colour development and absorbance readings were taken at 820 nm. ‡Continuous assay for pNPP and bis-pNPP hydrolysis at 405 nm. §End point assay for ONPG hydrolysis measurements at 420 nm.

Bond type		Substrate	PD-PTPRδ	PD-PTPRΩ
Ester	Monoester	*p*-Nitrophenyl phosphate†,‡	Yes	Yes
		Paraoxon‡	No	No
		Mioticol‡	No	No
		o-Phosphotyrosine†	Yes	Yes
		AMP†	No	No
		IMP†	No	No
		GMP†	No	No
		Pyridoxal 5′-phosphate†	No	No
	Diester	Bis(*p*-nitrophenyl) phosphate‡	Yes	Yes
		Tris(*p*-nitrophenyl) phosphate	No	No
		Tris(*p*-nitrobenzyl) phosphate	No	No
		Tetrakis(*p*-nitrophenyl) diphosphate	No	No
		NADP†	No	No
Glycosidic		*o*-Nitrophenyl β-D-galactoside§	Yes	Yes
		p-Nitrophenyl β-D-galactoside§	Yes	Yes
		p-Nitrophenyl β-D-glucuronide§	Yes	Yes
		p-Nitrophenyl α-D-glucoside§	Yes	Yes
		p-Nitrophenyl α-D-galactoside§	Yes	Yes
		p-Nitrophenyl *N*-acetyl-β-D-glucosaminide§	Yes	Yes
Peptide		H-Gly-PNA	No	No

(Table 1). The enzyme showed hydrolysis of *o*-phosphotyrosine alone. The reaction was initiated by addition of 58 nM enzyme and allowed to proceed for 5 min for phosphotyrosine at 37 °C. The reaction was quenched by addition of 20 μl of 70 % TCA. The reaction mixture was centrifuged at 9500 × ***g*** for 10 min, and the supernatant was added to 1 ml of Chen's reagent (3 M sulfuric acid, distilled water, 2.5 % ammonium molybdate and 10 % ascorbic acid mixed in 1:2:1:1 ratio). The reaction mixture was allowed to incubate at 37 °C for 30 min for colour stabilization. The absorbance was recorded at 820 nm (molar absorption coefficient is 25000 $M^{-1}\cdot cm^{-1}$) with a double beam Hitachi U-2010 UV–Vis spectrophotometer (Hitachi High Technologies America).

To determine the K_m and V_{max} for phosphotyrosine, the substrate was titrated and the resultant velocities plotted against substrate concentration. The data were fit to the Hill eqn (3)

$$d[P]/dt = (V_{max}X[S]^h)/\left([K]_{0.5}^h + [S]^h\right) \quad (3)$$

where $d[P]/dt$ is the velocity, V_{max} is the maximum velocity, [S] is the substrate concentration, $[K]_{0.5}$ is the substrate concentration at half maximal velocity and h is the Hill coefficient.

Pre-steady-state kinetics

The pre-steady-state kinetics for pNPP hydrolysis of PD-PTPRΩ was monitored in a double beam Hitachi U-2010 UV–Vis spectrophotometer with an appropriate blank given that the burst phase lasted for ∼50 s. Absorbance at $t = 0$ was subtracted from the rest of the data and absorbance plotted against time. Two measurements were averaged, and the data were fit to eqn (4)

$$A_{405} = v_s t + ((v_0 - v_s)/k)(1 - \exp^{(-kt)}) + c \quad (4)$$

where t is time in seconds, v_0 is initial velocity, v_s is steady-state velocity, k is the apparent pseudo-first-order rate constant for the transition from v_0 to v_s and c is the initial absorbance at 405 nm. Enzyme titration was carried out to ascertain whether the magnitude of burst increases with increasing enzyme concentration at 9.6–96.1 nM.

Inhibition kinetics

The inhibitory effect of phosphate and orthovanadate on the phosphomonoester hydrolysis activity of PD-PTPRδ and PD-PTPRΩ were assessed experimentally. Both the potency of the inhibitor and its affinity for the enzyme were computed by experimental IC_{50} determinations. IC_{50} determination assays were carried out in 100 mM HEPES pH 7.3, 5 mM pNPP and variable concentration of each inhibitor. The enzyme concentration was as specified above. Inhibitory potential of the covalent inhibitor NEM was also assessed on the phosphomonoester hydrolysis activity of protein tyrosine phosphatase Ω (PTPRΩ). The curves were fit to eqn (5), where I is the inhibitor concentration and y is the percentage of activity.

$$y = 100\%/[1 + (I/IC_{50})] \quad (5)$$

Furthermore, K_i^{app} were computed from the IC_{50} curves by fitting them to the quadratic Morrison eqn (6) for tight binding inhibition. This equation accounts for tight binding by doing away with the assumption that the free concentration of inhibitor equals the total concentration.

$$v_i/v_0 = 1 - \left(\left([E]_T + [I]_T + K_i^{app}\right) - \sqrt{\left([E]_T + [I]_T + K_i^{app}\right)^2 - 4[E]_T[I]_T}\right)/2[E]_T \quad (6)$$

Table 2 Summary of kinetic parameters of PD-PTPRδ and PD-PTPRΩ for various substrates

*Rate enhancement with respect to uncatalysed reaction. †The rate for spontaneous uncatalysed cleavage rates of diester bonds are 1×10^{-10} s. The value was obtained from Sasi et al. (2014) Int. J. Chem. Mol. Nucl. Mater. Metallurg. Eng. 8(9), 1010–1012. ‡The rate for spontaneous uncatalysed cleavage rates of glycosidic bonds in adenosine were obtained from Stockbride et al. (2010) Biorg. Chem. 38(5), 224–228 and are reported by comparing them with the sugar bond hydrolysis rates in our study. It should be pointed out that conventional glycoside hydrolases produce a rate enhancement of $\sim 10^{12}$. §The fits were unreliable with very wide confidence intervals given that the curve was not saturating (Figure 4D). ‖The fits were unreliable with very wide confidence intervals given that the curve was not saturating (Supplementary Figure S2C).

Substrate	Enzyme/s	K_m (mM)	V_{max} (nmol·min^{-1}·mg^{-1})	k_{cat} (min^{-1})	k_{cat}/K_m (mM^{-1}·min^{-1})	Rate enhancement*
pNPP	PD-PTPRδ	0.64 ± 0.1	154 ± 6	1.6	2.44	$\sim 10^{17}$
	PD-PTPRΩ (ss)	1.04 ± 0.3	3124 ± 243	2.0	1.92	$\sim 10^{17}$
	PD-PTPRΩ (bp)	1.56 ± 0.3	9330 ± 666	7.6	4.87	$\sim 10^{17}$
Bis-pNPP†	PD-PTPRδ§	NA	NA	NA	NA	NA
	PD-PTPRΩ(ss)	37.0 ± 4.7	10.96 ± 0.68	12.4	3.3×10^{-1}	$\sim 10^{9}$
oNPG‡	PD-PTPRδ	0.06 ± 0.01	0.47 ± 0.02	8.3×10^{-6}	1.4×10^{-4}	$\sim 10^{8}$
p-Tyr‖	PD-PTPRδ	NA	NA	NA	NA	NA

where v_i represents velocity in the presence of inhibitor, v_0 represents velocity in the absence of inhibitor, $[E]_T$ represents total enzyme, $[I]_T$ represents total inhibitor and K_i^{app} represents apparent K_i.

pH kinetics

The pH dependence of PTPRδ's phosphatase activity (k_{cat} and k_{cat}/K_m) and sugar hydrolase activity was monitored over the pH range 6.0–9.0. Pre-incubation of the enzyme in different pH buffers (5.5–8.5) did not cause any irreversible loss in activity. However, there was a minor loss of activity below pH 5.5 and hence the analysis was carried out only till pH 5.5. Thus, the inflections observed in the pH profile from 5.5 to 8.5 can be approximated to the true ionizations of the enzyme's catalytic groups. k_{cat} is the first-order rate constant. Its variation with pH is reflective of the ionization events in the catalytic complex. On the other hand, k_{cat}/K_m is the second-order rate constant indicative of ionization(s) of either the free substrate or the free enzyme towards the catalytic complex formation. The kinetic parameters, k_{cat} and k_{cat}/K_m obtained from each plot at different pH values were plotted as a function of pH to eqns (7) and (8) describing double and single ionization(s), respectively.

$$y = c/\{1 + ([H]/K_1) + (K_2/[H])\} \quad (7)$$

$$y = c/\{(1 + K_2/[H])\} \quad (8)$$

where y is the pH dependent parameter, c is the pH independent value of the parameter, [H] is the hydrogen ion concentration and K_1 and K_2 are the ionization constants for the ionizable groups involved in catalysis. pH of the assay mixture was adjusted with 50 mM mixed buffer (MES, PIPES and HEPES) and temperature kept constant at 25 °C.

Sugar hydrolysis assay

O-nitrophenyl β-galactopyranoside (ONPG), an analogue of lactose, is an artificial substrate used to assay the β-galactosidase activity of the enzyme. Since the reactions rates were slow, all the assays were carried out as endpoint measurements. Assays were initiated with the addition of enzyme to the test reactions. A blank reaction without the enzyme was maintained to normalize for non-catalytic hydrolysis of substrate. The quantity of the enzyme used varied depending on the length of incubation and the type of assay carried out. However, the enzyme concentration was kept constant between the test and the control for a given assay for ease of comparison. The reaction was terminated with the addition of 200 μl of Na_2CO_3. Liberated *O*-nitrophenol was measured at 420 nm. The amount of product formed was computed from the absorbance reading using an ε value of 4.5×10^3 M^{-1}·cm^{-1} [28]. Further, other artificial substrates *p*-nitrophenyl β-galactoside (PNPG), *p*-nitrophenyl β-glucuronide (PNPGlucu), *p*-nitrophenyl α-D-glucoside (4NGU-α), *p*-nitrophenyl α-D-galactoside (4NGA-α) and *p*-nitrophenyl *N*-acetyl-β-D glucosaminide (4NP-NA-GU) were also assessed for their hydrolysis by the PD-PTPRδ and PD-PTPRΩ (Table 1).

Binding assays

Differential scanning fluorimetry was carried out as described in previous studies [29–32]. Briefly, 10 μM protein was used and the extrinsic fluorophore dye Sypro-orange was employed to detect unfolding in the presence and absence of 100, 500 and 1000 μM small-molecule ligands.

RESULTS

Novel sugar hydrolase activity on the phosphatase domain of PTPRδ

It has been recently demonstrated that the library of native pockets is covered by a remarkably small number ($\sim$400) of representative pockets [9]. With that in mind, one might expect that basal enzymatic activity is an inherent feature of those pockets having an accidental juxtaposition of residues that have been demonstrated to have a role in catalysis [33,34]. Indeed, native like enzymatic pockets with catalytic residue types and geometries are reproduced in proteins lacking any selection for enzymatic function [9,10]. With these results in mind, we selected the PD-PTPRδ as the protein of interest. The protein was expressed and purified to homogeneity (Figure 1A). Systematic screens for hydrolase function, with phosphoester, glycosidic and peptide bond hydrolysis as representative activities were set up (Table 1). As the name implies, the PD-PTPRδ functions as a hydrolase that catalyses phosphomonoester hydrolysis of phosphorylated tyrosine residues on proteins. As expected, the protein showed good phosphatase activity as is evident in the hydrolysis of the artificial substrate *p*-nitrophenyl phosphatase, an analogue of phosphotyrosine (Figure 1B) (Table 2). Surprisingly, the protein also showed activity with the ONPG substrate. However, the

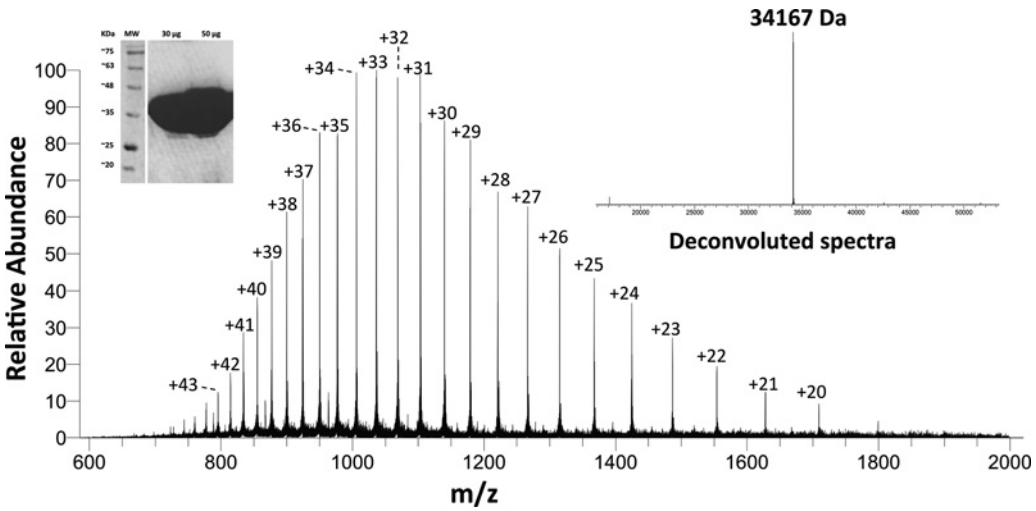

Figure 2 Mass spectrometric analysis of PD-PTPRδ

The mass spectrum depicts the isotope clusters of the various charged states for the intact protein obtained by direct infusion of the protein into a high-mass accuracy Q Exactive™ Plus mass spectrometer. The right and left insets depict the deconvoluted spectrum and the SDS/PAGE analysis with overloaded protein, respectively, as a means of assessing protein purity.

activity was much feebler than for the phosphomonoester bond hydrolysis (Figures 1C and 1D). ONPG is a mimic of lactose and is a substrate that is routinely employed for assaying β-galactosidase activity. To ensure that the observed activity is not an artifact, a close homologue of the protein, the PD-PTPRΩ, was expressed, purified to homogeneity and assayed for possible sugar hydrolase activity. PD-PTPRΩ shares 43.34 % sequence identity with PD-PTPRδ (Supplementary Figure S1A) and has the same overall global fold (Supplementary Figure S1B). As expected, PD-PTPRΩ also showed hydrolysis of ONPG (Figure 1D). However, PD-PTPRδ hydrolyses the sugar substrates ∼1.5- to 2-fold better than PD-PTPRΩ. The enzyme concentration dependence of sugar hydrolase activity for PD-PTPRδ showed a linear increase providing additional proof that the origin of the activity is in the purified recombinant protein (Supplementary Figure S1C). Since, among the three distinct substrate classes tested (Table 1), the enzyme hydrolysed both the phosphomonoester and the sugar substrates, it could be speculated that it is a non-specific hydrolase. However, both PD-PTPRδ and PD-PTPRΩ failed to show any discernible peptide hydrolysis activity even after incubating the substrate with repeated supplementation of high concentrations of enzyme every 12 h (Supplementary Figure S1D). All these experiments indicate that the sugar hydrolase activity indeed originates from the PD-PTPRδ and is highly specific for the hydrolysis of both glycosidic and phosphomonoester bonds.

It is understood that the purity of the protein preparation is a major criterion in such kind of studies as use of impure enzyme can lead to aberrant results. The mass and purity of the protein were assessed by overloading the protein on an SDS/PAGE gel and by carrying out mass spectrometric analysis (Figure 2). Mass spectrometric analysis can not only yield the protein's identity through comparison with the expected mass of the protein of interest, but also the relative purity of the sample based on the ratio of the desired mass peak to other mass peaks in the sample [35,36]. The intact mass was determined to be 34167 Da based on direct infusion into a high mass accuracy mass Q Exactive™ Plus mass spectrometer. This is in close agreement with the theoretical average mass of 34167.5 corresponding to the protein sequence with its N-terminal methionine cleaved. Further, the presence of the stereotypical isotope clusters of the various charge states with no other overlapping clusters suggests that no other contaminating proteins are present (Figure 2). The SDS/PAGE gel overloaded with 30 and 50 μg PD-PTPRδ also does not show any visible contaminants (Figure 2 inset). Further, it has to be noted that the activity was consistent across different batches of proteins purified and across two different proteins viz., PD-PTPRδ and PD-PTPRΩ tested.

The literature is replete with examples of catalytic promiscuity with the most prominent example being that of proteases (catalysing the hydrolysis of C—N bond) also carrying out ester (C—O) hydrolysis [37]. However, to the best of our knowledge, our example is the first instance of a single enzyme catalysing the hydrolysis of a COP bond and a COC bond.

Characterization of monoesterase activity of PD-PTPRδ and PD-PTPRΩ

Though the PDs of other PTPRs have been characterized, there are no studies that report the kinetic characterization of either PD-PTPRδ or PD-PTPRΩ. Detailed kinetic analysis was carried out to assess the hydrolysis of phosphorylated substrate by PD-PTPRδ and PD-PTPRΩ. Hydrolysis of the artificial substrate pNPP was monitored both in a continuous assay by monitoring *p*-nitrophenyl liberation and in an end point assay by monitoring for the liberated phosphate through Chen's assay [38]. As expected, the enzymes showed activity against pNPP with a rate enhancement of $\sim 10^{17}$ compared with the uncatalysed reaction (Table 2). This rate enhancement corresponds to that displayed by other phosphatases [39]. PD-PTPRΩ showed better pNPP hydrolysing activity than PD-PTPRδ; though the time-dependence of substrate to product conversion by PD-PTPRδ was linear, PD-PTPRΩ showed a biphasic plot indicative of a burst followed by a steady state (Figure 3A). Pre-steady-state kinetic analysis showed that the magnitude of the burst phase was dependent on protein concentration (Figures 3B and 3C) and

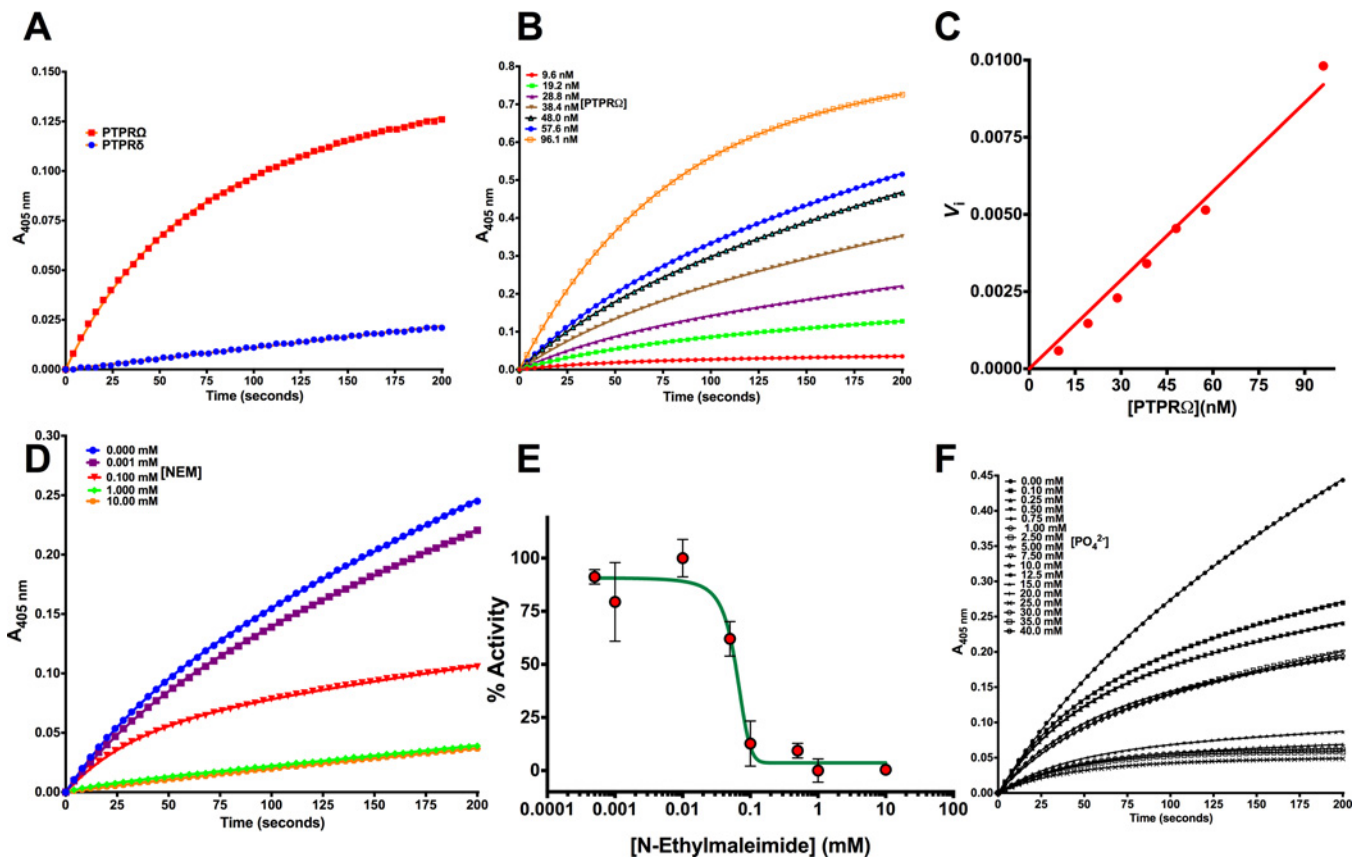

Figure 3 Hydrolysis of a phosphate substrate by PD-PTPRδ and PD-PTPRΩ

(**A**) The time dependence of activity for PD-PTPRδ and PD-PTPRΩ. (**B**) Enzyme concentration dependence of the burst phase magnitude for PD-PTPRΩ as visualized on the time course measurement of substrate to product conversion. (**C**) Replot of data from (B) as a function of PD-PTPRΩ concentration. (**D**) Time course measurement of PD-PTPRΩ activity as a function of NEM concentration, an irreversible inhibitor, showing vanishing burst phase. (**E**) Replot of % activity as a function of NEM concentration. (**F**) Time course measurement of PD-PTPRΩ activity as a function of phosphate concentration, a non-covalent reversible inhibitor, showing the retention of burst phase. The symbols represent experimental data points, and the line represents the non-linear least squares fit. The *y*-axis on panels (A, B, D and F) shows the absorbance measurements estimated at 405 nm for the conversion of pNPP to *p*-nitrophenol. The experimental data points were fit to the respective equations using the non-linear curve-fitting algorithm of GraphPad Prism v 6.0e or the software provided with Hitachi U-2010 UV–Vis spectrophotometer.

vanished with increasing *N*-ethylmaleimide (NEM) (Figure 3D). NEM is an irreversible inhibitor of enzymes with active site cysteine residues and is widely employed to probe the role of thiol groups in enzyme mechanism studies. Inhibition and the vanishing burst phase in the presence of NEM is indicative of the phosphocysteinyl intermediate hydrolysis being the rate-limiting step in PD-PTPRΩ (Figure 3E). PTPRs are known to employ a cysteine nucleophile to attack the incoming phosphorylated substrate to form the phosphoenzyme intermediate on the reaction coordinate. Sequence analysis and structural superposition of the various PTPRs showed that the motif HCXXGXGR, pivotal to catalysis and conserved across all the PTPs, is highly conserved in PD-PTPRΩ (Supplementary Figure S1A). It should be pointed out here that phosphate, which is a reversible inhibitor of the enzyme activity, does not abolish the burst phase (Figure 3F). The pNPP hydrolysing activity of the PTPRΩ and PTPRδ enzymes was inhibited by phosphate with mM IC_{50} values indicative of poor affinity for the active site (Supplementary Figure S2A). On the other hand, orthovanadate potently inhibited the pNPP hydrolysing activity of PTPRδ with a K_i^{app} of 120.1 ± 12.9 nM (Supplementary Figure S2B). Phosphotyrosine, when tested as substrate for PD-PTPRδ, did get hydrolysed but with very poor affinities (Supplementary Figure S2C and Table 2). Anchoring of the phosphotyrosine moiety on a peptide substrate of interest might be essential for efficient hydrolysis of the substrate. The tyrosine residue failed to inhibit the pNPP hydrolysing activity of either enzyme indicating that the absence of a phosphate moiety yields a metabolite with no affinity whatsoever for the active site of the two enzymes.

To further understand the specificity of the PTP active site, a range of phosphate monoesters were assessed to monitor their hydrolysis (Table 1). The substrates tested included different nucleoside monophosphates and pyridoxal phosphate. The enzymes did not show any detectable activity against the above substrates indicating that the active site is highly specific for the hydrolysis of their intended substrate.

The affinity and turnover of the substrate pNPP for PD-PTPRδ was assayed at several different pH values to understand the pH optima for the hydrolysis of the phosphorylated substrate. The plot of k_{cat} versus pH was a bell shaped curve with both acidic and alkaline limbs (Figure 4A). The pH dependence of k_{cat} of PD-PTPRδ towards the substrate pNPP indicated that one group must be unprotonated ($pK_a \sim 4.72$) and one group must be protonated ($pK_a \sim 7.4$) for effective catalysis. Similarly, the plot of k_{cat}/K_m also showed a reasonable fit to the equation for two ionizations, but did not converge to a good fit when the equation for single or triple ionization was employed (Figure 4B). However, the alkaline limb was more pronounced with a pK_a of ~ 6.65. The acidic

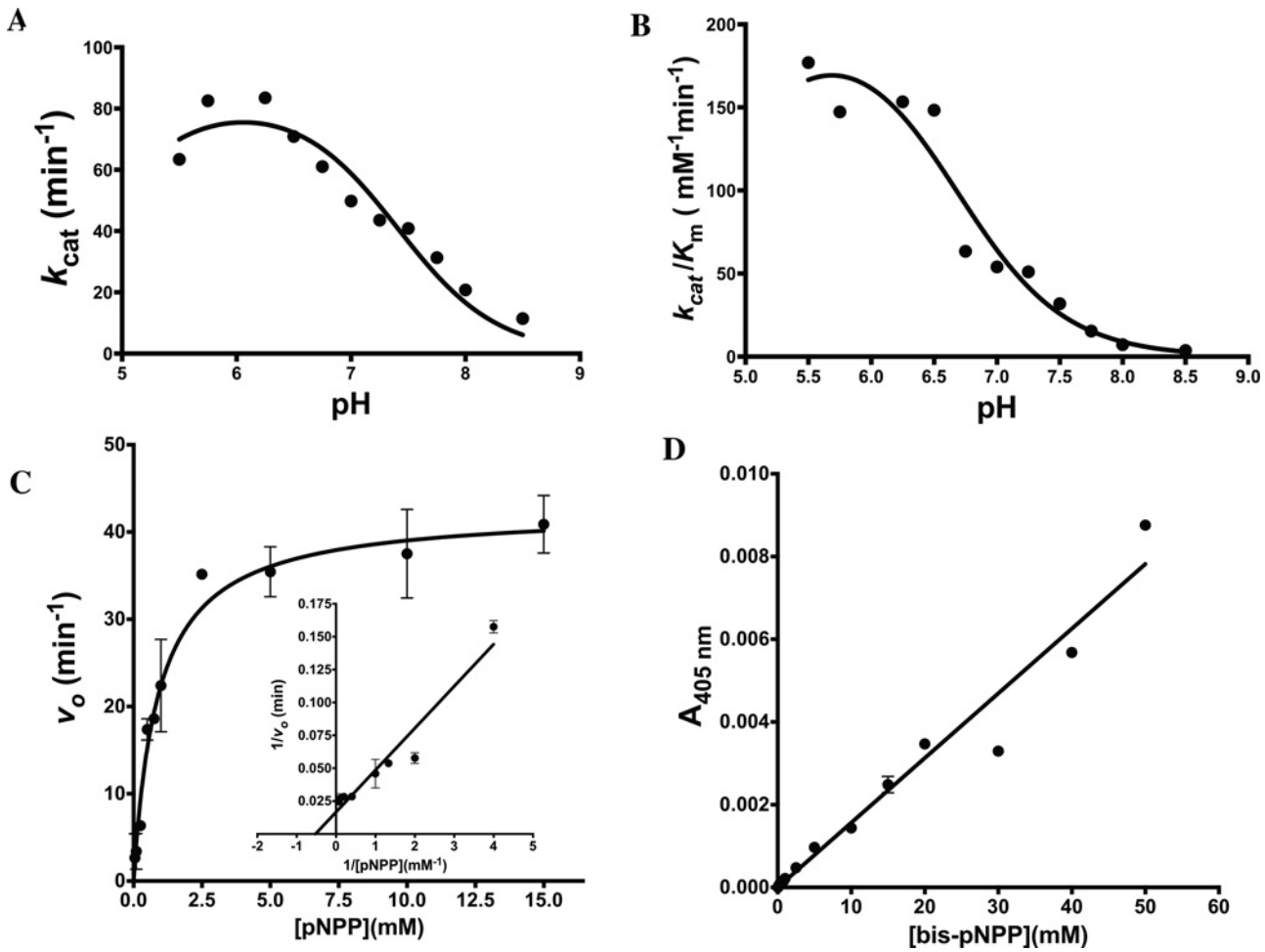

Figure 4 Characterization of phosphatase activity for PD-PTPRδ

(**A**) Plot of k_{cat} as a function of pH. (**B**) Plot of k_{cat}/K_m as a function of pH. (**C**) Substrate versus velocity plot for PD-PTPRδ hydrolysis of pNPP showing hyperbolic kinetics. Inset shows the double-reciprocal Lineweaver–Burk plot. (**D**) Substrate versus velocity plot for PD-PTPRδ hydrolysis of bis-pNPP showing non-saturating kinetics even at the high concentration of 50 mM bis-pNPP. The experimental data points were fit to their respective equations using the non-linear curve-fitting algorithm of GraphPad Prism v 6.0e.

limb lacked points due to possible enzyme denaturation below pH 5.5 (see Experimental). However, an approximation of the pK_a for the acidic limb gave an estimate of 4.72, similar to that obtained from the k_{cat} versus pH plot. This, once again, indicates that one group is likely unprotonated (p$K_a \sim 4.72$) and one group protonated (p$K_a \sim 6.65$) on either the substrate or the enzyme to enable effective catalytic complex formation. However, it should be noted here that the pK_a values presented for the acidic limb are mere extrapolations from the fits and should be considered as approximate estimates of the values.

In spite of the pH optima for activity being around pH 6.3, all phosphatase activity assays were performed at pH 7.3 in order to reduce the non-catalytic hydrolysis of the substrate. Table 2 summarizes the kinetic parameters, and Figure 4(C) and Supplementary Figure S2(D) show the substrate versus velocity plot of both PD-PTPRδ and PD-PTPRΩ for the phosphorylated substrate pNPP, respectively. The values of K_m and k_{cat} for PD-PTPRΩ were obtained from slopes taken both from the burst phase and the steady-state phase (Supplementary Figure S2D). As seen in the figure, PD-PTPRΩ shows substrate inhibition with pNPP that is absent from the substrate versus velocity plot for PD-PTPRδ. This differential behaviour can be exploited in the discovery of homologue specific inhibitors against the two enzymes.

Characterization of diesterase activity of PD-PTPRδ and PD-PTPRΩ

Monoesterases are highly specific for monoester hydrolysis and do not usually display diesterase activity. As an exception, alkaline phosphatase is known to display both monoesterase and diesterase activity [40]. However, the latter activity is far weaker than the principal activity of monoester hydrolysis. It came as a surprise when the PD-PTPRδ displayed diesterase activity on the artificial substrate bis-pNPP in spite of the highly discriminative nature of the active site towards a particular kind of phosphate monoester (Table 1). It should be pointed out that the diesterase activity was also detected with the close homologue PTPRΩ (Supplementary Figure S2E). Figure 4(D) shows the substrate versus velocity plot for bis-pNPP hydrolysis for PD-PTPRδ. However, the curve failed to saturate even at a high concentration of 60 mM making it difficult to estimate reliable kinetic parameters. The diesterase activity was also inhibited by NEM, once again implicating an active site cysteine in catalysing both monoesterase and diesterase

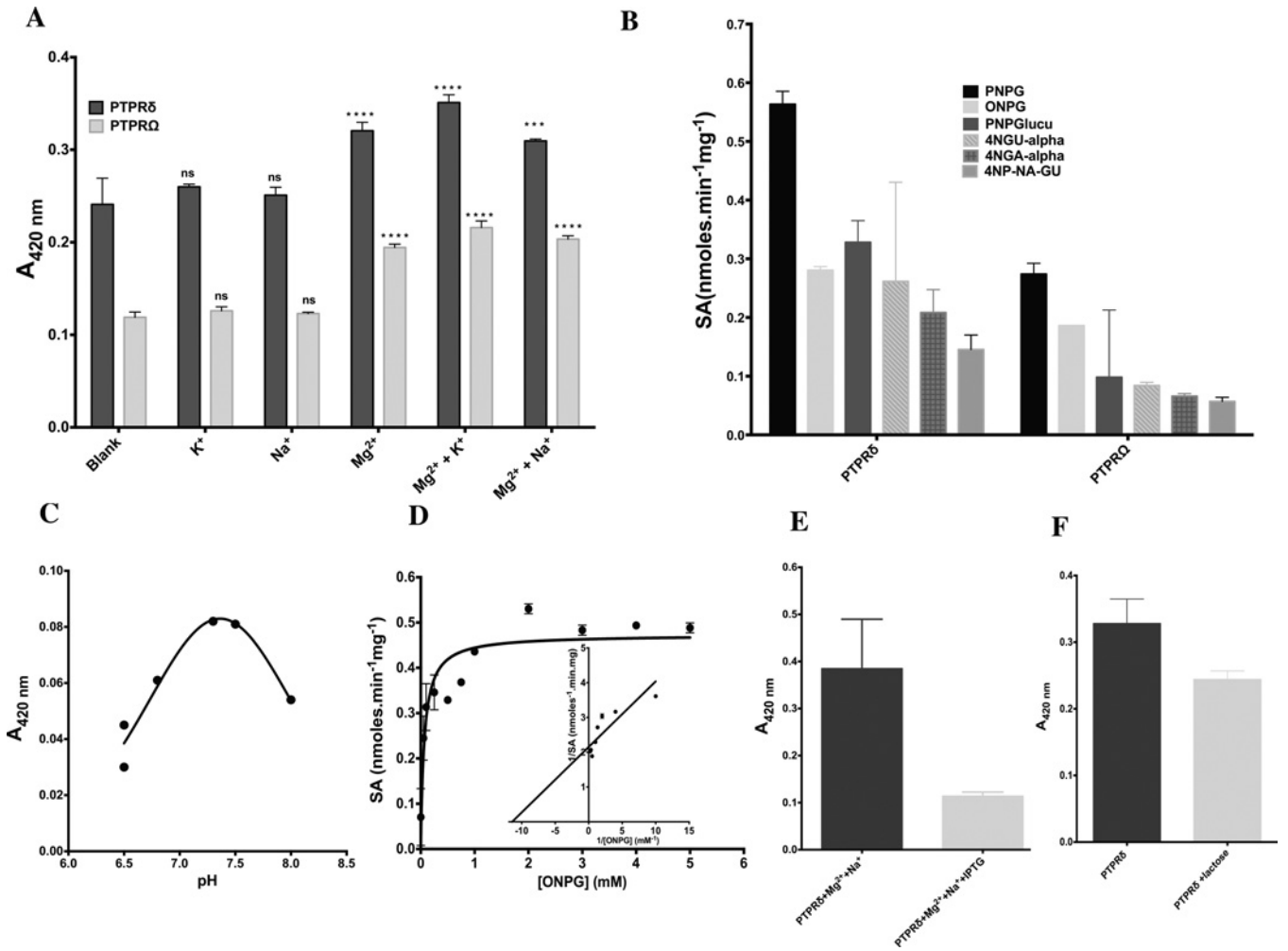

Figure 5 Characterization of sugar hydrolase activity for PD-PTPRδ and PD-PTPRΩ

(**A**) Metal-ion dependence for sugar hydrolase activity of PD-PTPRδ and PD-PTPRΩ. The pairwise two-way ANOVA was performed between the blank and the respective test pairs. '****' represents a P-value of <0.0001. (**B**) Screening of various sugar substrates to determine substrate discrimination across the PD-PTPRδ and PD-PTPRΩ. (**C**) pH dependence for sugar hydrolase activity of PD-PTPRδ as assessed for ONPG. (**D**) Substrate versus velocity plot for PD-PTPRδ hydrolysis of *o*-nitrophenyl galactoside showing hyperbolic kinetics. Inset shows the double-reciprocal Lineweaver–Burk plot. (**E**) Effect of IPTG and (**F**) lactose on the sugar hydrolysis activity of PD-PTPRδ. The experimental data points were fit to the respective equations using the linear and non-linear curve-fitting algorithm of GraphPad Prism v 6.0e.

activities from the same active site pocket (Supplementary Figure S4A). Moreover, this suggests that the enzyme displays substrate promiscuity. Designing of specific inhibitors for phosphatases has confounded medicinal chemists because of the high-conservation of the P-loop. Our findings, that the enzymes act on diesterases in addition to their primary role as monoester hydrolases and show different behaviour in hydrolysing their monoester substrates, assumes significance from the perspective of designing specific inhibitors for this class of enzymes.

A range of analogues of pNPP and bis-pNPP were assessed to see whether the enzyme could act on them given the promiscuity it displays towards monoester and diester hydrolysis. Supplementary Figure S3 shows the structures of the various analogues employed. It is interesting to note that the enzyme hydrolysed none of them. Further, they neither show inhibition of the phosphatase activity for pNPP hydrolysis nor did they bind to the enzyme as assessed by differential scanning fluorimetry. This indicates that the enzyme is intolerant to any substitutions on the phosphate group of either pNPP or bis-pNPP, and hence, binding of and activity on these substrates are mainly dependent on the presence of the phosphate group. This observation makes the activity shown on sugar substrates ONPG and PNPG by the enzymes all the more significant.

Characterization of sugar hydrolase activity of PD-PTPRδ and PD-PTPRΩ

Having confirmed the sugar hydrolysis activity as emerging from PD-PTPRδ and PD-PTPRΩ, we tested a range of sugars as possible substrates of the enzyme (Table 1). Before undertaking further kinetic characterization, the metal ion dependence of the sugar hydrolase activity was assessed (Supplementary Table S1 and Figure 5A). The sugar hydrolysis activity increases $\sim$1.5-fold in the presence of the divalent cation magnesium and monovalent cation potassium (Figure 5A). This dependence of the sugar hydrolysis activity on both the divalent and monovalent cation is highly similar to that shown by conventional sugar hydrolases [41]. It should be pointed out here that the phosphatase activity of the enzyme is independent of either divalent or monovalent metal

ions (Supplementary Figure S2F). However, phosphatases from the HAD superfamily are metal-dependent enzymes relying on the presence of divalent cations for catalysis of the phosphomonoester bond [42]. Assaying the various sugars indicated that PNPG was the best substrate followed by the other sugars (Figure 5B). The pH dependence of the sugar hydrolysis activity indicated a pH optimum of ∼7.3 (Figure 5C), which is markedly different from that displayed for the phosphatase activity (pH 6.3). Detailed kinetic characterization of the sugar hydrolase activity was not possible since the activity against sugar substrates was extremely slow and could not be carried out without resorting to a non-catalytic amount of the enzyme. However, we were able to assess the apparent affinity (K_m^{app}) and apparent maximum velocity (V_{max}^{app}) of the enzyme for the substrate ONPG by incubating the reaction with 1 μM enzyme at 37 °C for ∼19 h. The enzyme, under the conditions of the assay, showed conventional Michaelis–Menten hyperbolic behaviour in hydrolysing ONPG (Figure 5D). The sugar hydrolysing activity was markedly inhibited in the presence of IPTG and mildly inhibited with lactose, both structural analogues of the sugar substrates employed (Figures 5E and 5F). It should be pointed out that the assay was blind to the hydrolysis of lactose, if any, and only reported on the interference of ONPG hydrolysis activity by lactose. Further, it should be noted that IPTG did not interfere with the phosphomonoester hydrolysis activity of PD-PTPRδ (Supplementary Figure S4B). On the other hand, phosphate did not interfere with the sugar hydrolase activity even at 30 mM (Supplementary Figure S4C). However, NEM did show reduction in the sugar hydrolase activity (Supplementary Figure S4D). This inhibition could not be further assessed because of the extremely slow reaction rates and may be indicative of the involvement of cysteine either in catalysis or the binding of ONPG to enzyme.

DISCUSSION

Latent promiscuous enzyme activities might constitute an important pool of chemistries that might confound our understanding/modelling of metabolism. For instance, 37 % of the enzymes in *E. coli* genome show promiscuous activities and 65 % of the known metabolic reactions arise from such generalist enzymes [43]. The latter number represents a huge fraction of the total chemistries that take place in a cell, and unlike the way traditional enzymology is done, the emphasis of future enzymatic studies should be on the unravelling and characterization of such latent activities.

It has been shown in the past that substrate promiscuity is a far more frequent occurrence in a genome than catalytic promiscuity. Moreover, it has been argued that even in cases where catalytic promiscuity is seen there needs to be a common substrate substructure that might facilitate the binding and hence, catalysis i.e. an appropriate anchor group or chemophore might lead the substrate to bind to a larger, and often diverse, number of pockets with the right alignment of active site residues [44]. In fact, in a previous study from our group, we have demonstrated that the limited number of geometrical pockets that are present in biologically occurring proteins [9] suggests that promiscuity should be the rule rather than exception. Given the small fraction of amino acids that are usually found in the active sites of enzymes and the high probability of their co-occurrence in other pockets [9,10,33,34], led us to conclude that promiscuous activities ought to be more widespread than was previously assumed.

As an important case study with possible implications for the physiological functionality of the protein, we have demonstrated a novel sugar hydrolase activity for PD-PTPRδ and PD-PTPRΩ. The finding assumes significance because of the crucial role these phosphatases play in the signal transduction pathways of neuronal growth. Further, demonstration of catalytic promiscuity (as in the hydrolysis of COC bond apart from the usual COP bond) and substrate promiscuity (hydrolysis of substrates with diester bonds as well as monoester bonds) yet retaining substrate discrimination is indicative of the fine balance that determines promiscuity versus specificity even when catalysing diverse reactions. It can be speculated that the common nitrophenyl anchor group might have contributed to the recognition across the three substrate types. However, as demonstrated with substrate analogues for pNPP and bis-pNPP that do not act as either substrates or inhibitors (Supplementary Figure S3), it is highly unlikely that the nitrophenol moiety might be the determinant for either binding or catalysis. This assumption is further confirmed due to the lack of inhibition of pNPP hydrolysis activity shown by the tyrosine residue. Marked differences in the rates and conditions of catalysis render these reactions unique and specific (Figure 6). For instance, though the phosphatase reaction is inhibited by phosphate and orthovanadate, they do not have any effect on the sugar hydrolysis activity of the enzyme. Further, IPTG affects sugar hydrolysis activity with no interference whatsoever in the phosphatase reaction. The differential metal ion dependence for the two activities constitutes another important difference that indicates differential mechanistic details for the two reactions. These differences led us to speculate that the activities might be emerging from two distinct pockets on the protein. We call such enzymes dizymes and posit that they will be important in regulation of cellular metabolism. If the product of one active site modulates the enzymatic behaviour of the other site, then having both chemistries in the same domain may exert local biochemical control in a cellular context.

To the best of our knowledge, this is the first study that shows both substrate promiscuity and catalytic promiscuity in an enzyme domain. Yet, the enzyme demonstrates discrimination and specificity in catalysing the hydrolysis of monoester and diester substrates. These promiscuous functionalities assume more significance in the light of PTPRδ's important role in neuronal development and its significant sequence identity with PTPRσ (a closely related phosphatase with ∼85 % sequence identity) and leucocyte common antigen related protein (LAR) that have been implicated in several malignancies and life-style disorders [45–47]. It has to be noted here that a lot of their role in neuronal processes stems from the ability of their extracellular domains to interact with proteoglycans, which are degraded intracellularly, and the promiscuous activity displayed by the intracellular PD may not be of mere interest in understanding the underlying mechanistic details but may have real physiological roles [48–51].

The order-of-magnitude differences in the rates of hydrolysis across the monoesterase, diesterase and glycosidic bond hydrolysis activities may indicate that the poor activities might possibly represent evolutionary repositories for future enzymatic functions. However, it has not escaped our notice that the physiologically relevant substrates may not have been assayed and in spite of our broad screen across three different substrate classes and two enzymes, we may have missed the preferred sugar and diesterase substrates that the enzyme acts upon in the cellular milieu. However, it would be a difficult task to assay all possible substrates that possess a COC bond or a diester bond given the myriad number of leaving groups that might require different assay systems for detection. For instance, the presence of COC bonds across various sugars and O-linked glycoproteins makes it a daunting task to devise specific assays for a single study. However, we believe that our study and its findings pave the way

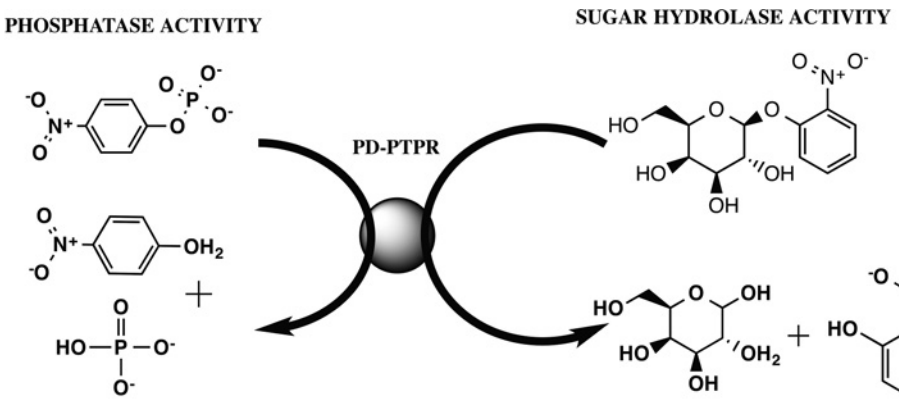

FACTORS	PHOSPHATASE	SUGAR HYDROLASE
CHEMISTRY	COP BOND CLEAVAGE	COC BOND CLEAVAGE
RATE ENHANCEMENT	~10^{17}	~10^{9}
DIVALENT/MONOVALENT METAL ION	NO EFFECT	ACTIVATOR METAL-DEPENDENT ACTIVITY
pH OPTIMA	6.3	7.3
IPTG	NO EFFECT	INHIBITOR
PHOSPHATE	INHIBITOR	NO EFFECT

Figure 6 Salient differences between the phosphatase and sugar hydrolase activity of PD-PTPRδ and PD-PTPRΩ

IPTG stands for isopropyl-β-D-1-thiogalactopyranoside and rate enhancement refers to the increase in the rate of a reaction vis-à-vis the uncatalysed rate. The structure files were downloaded from PubChem and the figure was rendered with ChemBioDraw 14.0.

for future enquiries into possible substrate preferences for these enzymes.

Design of specific inhibitors for phosphatases has been another challenging research area. The high conservation of the active site across the various phosphatases often leads to extensive non-specificity for the designed inhibitor rendering it clinically irrelevant [52]. Another important insight that emerges from our study is the differences between PD-PTPRδ and PD-PTPRΩ that could be potentially exploited in designing specific inhibitors for the respective phosphatase. PD-PTPRΩ shows rate-limiting phosphocysteinyl hydrolysis leading to a biphasic time-dependence of substrate to product conversion. The absence of this detectable rate-limiting step in PD-PTPRδ combined with the significant difference in the velocity of hydrolysis for pNPP and the sugar substrate for the two proteins indicate avenues that could be further utilized for discovery of specific inhibitors. Another difference is the substrate inhibition seen with PD-PTPRΩ that is absent in PD-PTPRδ. Substrate inhibition like behaviour usually arises because of an alternate site of binding and is possibly indicative of a novel pocket distinct from the active site that could be targeted for drug-discovery purposes.

In summary, the present study is the first to report the multiple distinct chemistries that are catalysed by the phosphatase domain of PD-PTPRδ and PD-PTPRΩ. The chemistries fall into the domain of both substrate promiscuity and catalytic promiscuity. Further, we also demonstrate convincing differences between the two closely related phosphatases that can be exploited to design specific inhibitors for the respective phosphatases. In conclusion, we posit that occurrence of promiscuous activities on enzymes is the rule rather than the exception and systematic screens to unravel such interactions would facilitate a better understanding of metabolism. This conclusion stems from the important insights provided by previous studies from our group linking the physics of protein folding and the presence of background biochemical activities [9,10,53,54]. In those studies, comparison of artificially generated compact protein structures (ART protein library) selected for thermodynamic stability but not for function, demonstrates that a remarkable number of properties of the native-like proteins are recapitulated. These include the complete set of small molecule ligand-binding pockets and most protein-protein interfaces. ART structures are predicted to weakly bind metabolites that are components of a significant fraction of metabolic pathways, with the most enriched pathway being glycolysis. Native-like active sites are also found in ART proteins. Overall, it appears that biochemical function is an intrinsic feature of proteins which Nature has significantly optimized during evolution. As an extension of this hypothesis, the current study presents the first experimental evidence for the presence of such random background activity by the demonstration of sugar hydrolase activity on the phosphatase domain of PD-PTPRδ and PD-PTPRΩ.

AUTHOR CONTRIBUTION

Bharath Srinivasan conceived of the study, participated in its design, carried out the experiments, analysed and interpreted the results and drafted the manuscript. Hanna Marks, Sreyoshi Mitra and David Smalley carried out the experiments. Jeffrey Skolnick

conceived of the study, participated in its design and coordination, provided appropriate resources, helped analyse the data and was involved in drafting and critically reviewing the manuscript. All authors read and approved the final manuscript.

ACKNOWLEDGEMENTS

We thank DNASU for providing the expression plasmids for clones of PD-PTPRδ and PD-PTPRΩ. We also thank the Developmental Therapeutics Program of the National Cancer Institute for providing the small molecules used in this study.

FUNDING

This work was supported by the Division of General Medical Sciences of the NIH [grant number GM-48835].

REFERENCES

1 Pandya, C., Farelli, J.D., Dunaway-Mariano, D. and Allen, K.N. (2014) Enzyme promiscuity: engine of evolutionary innovation. J. Biol. Chem. **289**, 30229–30236 CrossRef PubMed
2 Babtie, A., Tokuriki, N. and Hollfelder, F. (2010) What makes an enzyme promiscuous? Curr. Opin. Chem. Biol. **14**, 200–207 CrossRef
3 Khersonsky, O., Roodveldt, C. and Tawfik, D.S. (2006) Enzyme promiscuity: evolutionary and mechanistic aspects. Curr. Opin. Chem. Biol. **10**, 498–508 CrossRef PubMed
4 O'Brien, P.J. and Herschlag, D. (1999) Catalytic promiscuity and the evolution of new enzymatic activities. Chem. Biol. **6**, R91–R105 CrossRef PubMed
5 Jensen, R.A. (1976) Enzyme recruitment in evolution of new function. Annu. Rev. Microbiol. **30**, 409–425 CrossRef PubMed
6 Srinivasan, B., Kempaiah Nagappa, L., Shukla, A. and Balaram, H. (2015) Prediction of substrate specificity and preliminary kinetic characterization of the hypothetical protein PVX_123945 from *Plasmodium vivax*. Exp. Parasitol. 56–63
7 Glasner, M.E., Gerlt, J.A. and Babbitt, P.C. (2006) Evolution of enzyme superfamilies. Curr. Opin. Chem. Biol. **10**, 492–497 CrossRef PubMed
8 Kazlauskas, R.J. (2005) Enhancing catalytic promiscuity for biocatalysis. Curr. Opin. Chem. Biol. **9**, 195–201 CrossRef PubMed
9 Skolnick, J., Gao, M. and Zhou, H. (2014) On the role of physics and evolution in dictating protein structure and function. Israel J. Chem. **54**, 1176–1188 CrossRef
10 Skolnick, J., Gao, M. and Zhou, H. (2016) How special is the biochemical function of native proteins? F1000Res. **5**, 207 CrossRef
11 Rye, C.S. and Withers, S.G. (2000) Glycosidase mechanisms. Curr. Opin. Chem. Biol. **4**, 573–580 CrossRef PubMed
12 Zechel, D.L. and Withers, S.G. (2000) Glycosidase mechanisms: anatomy of a finely tuned catalyst. Acc. Chem. Res. **33**, 11–18 CrossRef PubMed
13 Tiganis, T. and Bennett, A.M. (2007) Protein tyrosine phosphatase function: the substrate perspective. Biochem. J. **402**, 1–15 CrossRef PubMed
14 Ensslen-Craig, S.E. and Brady-Kalnay, S.M. (2004) Receptor protein tyrosine phosphatases regulate neural development and axon guidance. Dev. Biol. **275**, 12–22 CrossRef PubMed
15 Stepanek, L., Stoker, A.W., Stoeckli, E. and Bixby, J.L. (2005) Receptor tyrosine phosphatases guide vertebrate motor axons during development. J. Neurosci. **25**, 3813–3823 CrossRef PubMed
16 Gonzalez-Brito, M.R. and Bixby, J.L. (2006) Differential activities in adhesion and neurite growth of fibronectin type III repeats in the PTP-delta extracellular domain. Int. J. Dev. Neurosci. **24**, 425–429 CrossRef PubMed
17 Uetani, N., Kato, K., Ogura, H., Mizuno, K., Kawano, K., Mikoshiba, K., Yakura, H., Asano, M. and Iwakura, Y. (2000) Impaired learning with enhanced hippocampal long-term potentiation in PTPdelta-deficient mice. EMBO J. **19**, 2775–2785 CrossRef PubMed
18 Shen, Y., Tenney, A.P., Busch, S.A., Horn, K.P., Cuascut, F.X., Liu, K., He, Z., Silver, J. and Flanagan, J.G. (2009) PTPsigma is a receptor for chondroitin sulfate proteoglycan, an inhibitor of neural regeneration. Science **326**, 592–596 CrossRef PubMed
19 Swarup, V.P., Mencio, C.P., Hlady, V. and Kuberan, B. (2013) Sugar glues for broken neurons. Biomol. Concepts **4**, 233–257 CrossRef PubMed
20 Altschul, S.F., Madden, T.L., Schaffer, A.A., Zhang, J., Zhang, Z., Miller, W. and Lipman, D.J. (1997) Gapped BLAST and PSI-BLAST: a new generation of protein database search programs. Nucleic Acids Res. **25**, 3389–3402 CrossRef PubMed
21 Notredame, C., Higgins, D.G. and Heringa, J. (2000) T-Coffee: a novel method for fast and accurate multiple sequence alignment. J. Mol. Biol. **302**, 205–217 CrossRef PubMed
22 Kumar, S., Tamura, K. and Nei, M. (2004) MEGA3: integrated software for molecular evolutionary genetics analysis and sequence alignment. Brief. Bioinform. **5**, 150–163 CrossRef PubMed
23 Guex, N. and Peitsch, M.C. (1997) SWISS-MODEL and the Swiss-PdbViewer: an environment for comparative protein modeling. Electrophoresis **18**, 2714–2723 CrossRef PubMed
24 Collaborative Computational Project, N (1994) The CCP4 suite: programs for protein crystallography. Acta Crystallogr. D Biol. Crystallogr. **50** Pt 5, 760–763 CrossRef PubMed
25 Laemmli, U.K. (1970) Cleavage of structural proteins during the assembly of the head of bacteriophage T4. Nature **227**, 680–685 CrossRef PubMed
26 Bradford, M.M. (1976) A rapid and sensitive method for the quantitation of microgram quantities of protein utilizing the principle of protein-dye binding. Anal. Biochem. **72**, 248–254 CrossRef PubMed
27 Gottlin, E.B., Xu, X., Epstein, D.M., Burke, S.P., Eckstein, J.W., Ballou, D.P. and Dixon, J.E. (1996) Kinetic analysis of the catalytic domain of human cdc25B. J. Biol. Chem. **271**, 27445–27449 CrossRef PubMed
28 Becerra, M., Cerdan, E. and Gonzalez Siso, M.I. (1998) Dealing with different methods for *Kluyveromyces lactis* beta-galactosidase purification. Biol. Proced. Online **1**, 48–58 CrossRef PubMed
29 Roy, A., Srinivasan, B. and Skolnick, J. (2015) PoLi: a virtual screening pipeline based on template pocket and ligand similarity. J. Chem. Inf. Model. **55**, 1757–1770 CrossRef PubMed
30 Srinivasan, B. and Skolnick, J. (2015) Insights into the slow-onset tight-binding inhibition of *Escherichia coli* dihydrofolate reductase: detailed mechanistic characterization of pyrrolo [3,2-f] quinazoline-1,3-diamine and its derivatives as novel tight-binding inhibitors. FEBS J. **282**, 1922–1938 CrossRef PubMed
31 Srinivasan, B., Tonddast-Navaei, S. and Skolnick, J. (2015) Ligand binding studies, preliminary structure–activity relationship and detailed mechanistic characterization of 1-phenyl-6,6-dimethyl-1,3,5-triazine-2,4-diamine derivatives as inhibitors of *Escherichia coli* dihydrofolate reductase. Eur. J. Med. Chem. **103**, 600–614 CrossRef PubMed
32 Srinivasan, B., Zhou, H., Kubanek, J. and Skolnick, J. (2014) Experimental validation of FINDSITE(comb) virtual ligand screening results for eight proteins yields novel nanomolar and micromolar binders. J. Cheminform. **6**, 16 CrossRef PubMed
33 Bartlett, G.J., Porter, C.T., Borkakoti, N. and Thornton, J.M. (2002) Analysis of catalytic residues in enzyme active sites. J. Mol. Biol. **324**, 105–121 CrossRef PubMed
34 Holliday, G.L., Almonacid, D.E., Mitchell, J.B. and Thornton, J.M. (2007) The chemistry of protein catalysis. J. Mol. Biol. **372**, 1261–1277 CrossRef PubMed
35 Acker, M.G. and Auld, D.S. (2014) Considerations for the design and reporting of enzyme assays in high-throughput screening applications. Perspect. Sci. **1**, 56–73 CrossRef
36 Scott, J.E. and Williams, K.P. (2004) Validating identity, mass purity and enzymatic purity of enzyme preparations. In Assay Guidance Manual (Sittampalam, G.S., Coussens, N.P., Nelson, H., Arkin, M., Auld, D., Austin, C., Bejcek, B., Glicksman, M., Inglese, J., Iversen, P.W. et al., eds), Eli Lilly & Company and the National Center for Advancing Translational Sciences, Bethesda, MD
37 Bornscheuer, U.T. and Kazlauskas, R.J. (2004) Catalytic promiscuity in biocatalysis: using old enzymes to form new bonds and follow new pathways. Angew. Chem. Int. Ed. Engl. **43**, 6032–6040 CrossRef PubMed
38 Chen, Jr, P.S., Toribara, T.Y. and Warner, H. (1956) Microdetermination of phosphorous. Anal. Chem. **28**, 1756–1758 CrossRef
39 Zalatan, J.G. and Herschlag, D. (2006) Alkaline phosphatase mono- and diesterase reactions: comparative transition state analysis. J. Am. Chem. Soc. **128**, 1293–1303 CrossRef PubMed
40 O'Brien, P.J. and Herschlag, D. (2001) Functional interrelationships in the alkaline phosphatase superfamily: phosphodiesterase activity of Escherichia coli alkaline phosphatase. Biochemistry **40**, 5691–5699 CrossRef PubMed
41 Juers, D.H., Matthews, B.W. and Huber, R.E. (2012) LacZ beta-galactosidase: structure and function of an enzyme of historical and molecular biological importance. Protein Sci. **21**, 1792–1807 CrossRef PubMed
42 Srinivasan, B., Forouhar, F., Shukla, A., Sampangi, C., Kulkarni, S., Abashidze, M., Seetharaman, J., Lew, S., Mao, L., Acton, T.B. et al. (2014) Allosteric regulation and substrate activation in cytosolic nucleotidase II from Legionella pneumophila. FEBS J. **281**, 1613–1628 CrossRef PubMed
43 Nam, H., Lewis, N.E., Lerman, J.A., Lee, D.H., Chang, R.L., Kim, D. and Palsson, B.O. (2012) Network context and selection in the evolution to enzyme specificity. Science **337**, 1101–1104 CrossRef PubMed
44 Khersonsky, O., Malitsky, S., Rogachev, I. and Tawfik, D.S. (2011) Role of chemistry versus substrate binding in recruiting promiscuous enzyme functions. Biochemistry **50**, 2683–2690 CrossRef PubMed
45 Jacob, S.T. and Motiwala, T. (2005) Epigenetic regulation of protein tyrosine phosphatases: potential molecular targets for cancer therapy. Cancer Gene Ther. **12**, 665–672 CrossRef PubMed
46 Julien, S.G., Dube, N., Hardy, S. and Tremblay, M.L. (2011) Inside the human cancer tyrosine phosphatome. Nat. Rev. Cancer. **11**, 35–49 CrossRef PubMed

47 Chagnon, M.J., Uetani, N. and Tremblay, M.L. (2004) Functional significance of the LAR receptor protein tyrosine phosphatase family in development and diseases. Biochem. Cell Biol. **82**, 664–675 CrossRef PubMed
48 Davies, M., Thomas, G.J., Shewring, L.D. and Mason, R.M. (1992) Mesangial cell proteoglycans: synthesis and metabolism. J. Am. Soc. Nephrol. **2** 10 Suppl, S88–S94 PubMed
49 Bienkowski, M.J. and Conrad, H.E. (1984) Kinetics of proteoheparan sulfate synthesis, secretion, endocytosis, and catabolism by a hepatocyte cell line. J. Biol. Chem. **259**, 12989–12996 PubMed
50 Owens, R.T. and Wagner, W.D. (1991) Metabolism and turnover of cell surface-associated heparan sulfate proteoglycan and chondroitin sulfate proteoglycan in normal and cholesterol-enriched macrophages. Arterioscler. Thromb. **11**, 1752–1758 CrossRef PubMed
51 Fedarko, N.S., Termine, J.D., Young, M.F. and Robey, P.G. (1990) Temporal regulation of hyaluronan and proteoglycan metabolism by human bone cells *in vitro*. J. Biol. Chem. **265**, 12200–12209 PubMed
52 Zhang, Z.Y. (2002) Protein tyrosine phosphatases: structure and function, substrate specificity, and inhibitor development. Annu. Rev. Pharmacol. Toxicol. **42**, 209–234 CrossRef PubMed
53 Skolnick, J. and Gao, M. (2013) Interplay of physics and evolution in the likely origin of protein biochemical function. Proc. Natl. Acad. Sci. U.S.A. **110**, 9344–9349 CrossRef PubMed
54 Skolnick, J., Gao, M., Roy, A., Srinivasan, B. and Zhou, H. (2015) Implications of the small number of distinct ligand binding pockets in proteins for drug discovery, evolution and biochemical function. Bioorg. Med. Chem. Lett. **25**, 1163–1170 CrossRef PubMed

Received 4 April 2016/12 May 2016; accepted 16 May 2016
Accepted Manuscript online 17 May 2016, doi:10.1042/BCJ20160289